Eur. Phys. J. C 18, 283–292 (2000)
Digital Object Identifier (DOI) 10.1007/s100520000540

THE EUROPEAN PHYSICAL JOURNAL C

On the investigation of possible systematics in WIMP annual modulation search

R. Bernabei[1], P. Belli[1], R. Cerulli[1], F. Montecchia[1], M. Amato[2], G. Ignesti[2], A. Incicchitti[2], D. Prosperi[2], C.J. Dai[3], H.L. He[3], H.H. Kuang[3], J.M. Ma[3]

[1] Dipartimento di Fisica, Universita' di Roma "Tor Vergata" and INFN, sez. Roma2, 00133 Rome, Italy
[2] Dipartimento di Fisica, Universita' di Roma "La Sapienza" and INFN, sez. Roma, 00185 Rome, Italy
[3] IHEP, Chinese Academy, P.O. Box 918/3, Beijing 100039, P.R. China

Received: 26 September 2000 / Published online: 27 November 2000 – © Springer-Verlag 2000

Abstract. An investigation of the WIMP annual modulation signature is in progress at the Gran Sasso National Laboratory of the I.N.F.N. by means of the $\simeq 100$ kg NaI(Tl) DAMA set-up; the results obtained during four annual cycles have already been published. In this paper we will further address in some details the main arguments, which have allowed us to exclude known systematic effects as a possible source of the annual modulation observed in the rate at very low energy. In particular, the (more recently released) data of the DAMA/NaI-3 and DAMA/NaI-4 running periods are considered as quantitative examples.

1 Introduction

The existence of weakly interacting massive particles (WIMPs) as relics from the early Universe is required by both experimental observations and cosmological models. According to the more widely considered description, they would be gravitationally trapped in the galactic halo with a Maxwellian velocity distribution having a cut-off at the galactic escape velocity and, therefore, they would continuously cross the Earth. These particles can be detected deep underground by investigating their elastic scatterings on the target nuclei of a suitable set-up. The nuclear recoil energy in the keV range is the measured quantity and a quasi-exponential shape is expected for the energy distribution of the recoil events.

As is known, to overcome the intrinsic uncertainties which exist in the comparison of the results achieved by different experiments (even more when different target nuclei and/or different techniques are used) and to be able to identify the presence of a possible signal, experiments with a proper signature are necessary. For various reasons, only the so-called annual modulation signature (first discussed in [1,2]) can be exploited in practice. This is based on the fact that, since the Earth turns round the Sun, it would be crossed by a larger WIMP flux in June (when its rotational velocity adds up to the velocity of the whole solar system in the Galaxy) and by a smaller flux in December (when the two velocities are in opposite directions), inducing a peculiar modulation of the measured low energy counting rate.

As we have already pointed out, the annual modulation signature is very distinctive [3–7]. In fact, a WIMP-induced seasonal effect must simultaneously satisfy all the following requirements: the rate must contain a component modulated according to a cosine function (1) with one year period (2) and a phase that peaks around $\simeq 2$ June (3); this modulation must only be found in a well-defined low energy range, where WIMP-induced recoils can be present (4); it must apply to those events in which just one detector of many actually "fires" (single hit events), since the WIMP multi-scattering probability is negligible (5); the modulation amplitude in the region of maximal sensitivity must be $\lesssim 7\%$ peak to peak (6). Only systematic effects able to fulfill these six requirements could fake this signature; therefore for some other effect to mimic such a signal is highly unlikely.

Table 1. Released data sets

Period	Statistics (kg day)	Reference
DAMA/NaI-1	4549	[4]
DAMA/NaI-2	14962	[5]
DAMA/NaI-3	22455	[7]
DAMA/NaI-4	16020	[7]
Total statistics	57986	[7]
+ DAMA/NaI-0	limits on recoils fraction by PSD	[8]

Results on the data collected during four annual cycles (see Table 1[1]) have been released so far [4,5,7].

[1] We list also the DAMA/NaI-0 running period since this has been included in the particular model dependent search for a candidate performed in [7]. These data were analysed in terms of pulse shape discrimination (PSD) obtaining an upper limit on the recoil rate [8]

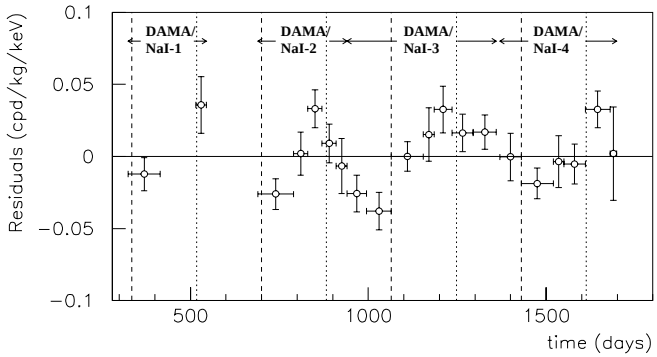

Fig. 1. Model independent residual rate for single hit events, in the 2–6 keV cumulative energy interval, as a function of the time elapsed since January 1 of the first year of data taking. The expected behaviour of a WIMP signal is a cosine function with minimum roughly at the dashed vertical lines and with maximum roughly at the dotted ones [7]

The model independent approach on these four annual cycles (57986 kg day statistics) offers immediate evidence for the presence of an annual modulation of the rate of the single hit events in the lowest energy interval (2–6 keV) as shown in Fig. 1 [7]. In fact, the χ^2 test on the data of Fig. 1 disfavors the hypothesis of unmodulated behaviour (probability: $4 \cdot 10^{-4}$); while fitting these residuals with the function $A \cdot \cos\omega(t - t_0)$, one gets

(i) for the period $T = 2\pi/\omega = (1.00 \pm 0.01)$ year when t_0 is fixed at the 152.5th day of the year (corresponding to $\simeq$ 2 June);
(ii) for the phase $t_0 = (144 \pm 13)$ days, when T is fixed at 1 year. In the two cases A is (0.022 ± 0.005) cpd/kg/keV and (0.023 ± 0.005) cpd/kg/keV, respectively. Similar results, but with slightly larger errors, are found in case all the parameters are kept free. In conclusion, the presence of an annual modulation in the residual rate of the single hit events in the lowest energy interval (2–6 keV) with features expected for a WIMP signal is supported by the data [4–7].

In the following, the careful investigation of known systematic effects is discussed in some details; no systematic effect able to mimic such a signature has been found so far.

2 Brief summary on the experimental set-up

The investigation of the annual modulation signature is performed by using the $\simeq$ 100 kg NaI(Tl) DAMA set-up. The detailed description of this set-up, of its radiopurity, of its performance, of the used hardware procedures and of the data reduction has been given in [3]. Here we only recall that the detectors used in the annual modulation studies are nine 9.70 kg NaI(Tl) scintillators especially built for this purpose. The bare NaI(Tl) crystals are encapsulated in suitably radiopure Cu housings; 10 cm long Tetrasil-B light guides act as optical windows on the two end faces of the crystals and are coupled to EMI9265-B53/FL photomultipliers (PMT). The two PMTs work in coincidence and collect light at the single photoelectron threshold; the measured light response is 5.5–7.5 photoelectrons/keV depending on the detector [3]. The software energy threshold has been cautiously taken at 2 keV [3–5, 7,8]. The detectors are inside a low radioactivity sealed copper box installed in the center of a low radioactivity Cu/Pb/Cd-foils/polyethylene/paraffin shield. The copper box is maintained in a high purity (HP) nitrogen atmosphere in slight overpressure with respect to the external environment. Furthermore, also the whole shield is sealed and maintained in the HP nitrogen atmosphere. The entire installation is air-conditioned. On the top of the shield a glove-box (also maintained in the HP nitrogen atmosphere) is directly connected to the inner Cu box, housing the detectors, through Cu pipes. The pipes are filled with low radioactivity Cu bars which can be removed to allow the insertion of radioactive sources for calibrating the detectors in the same running condition, without any contact with external air. In the production runs, the knowledge of the energy scale is assured by periodical calibrations with the ^{241}Am source and by monitoring (in the production data themselves summed every $\simeq$ 7 days) the position and resolution of the 46.5 keV γ line of the ^{210}Pb [3–5,7,8]. The latter peak is present at the level of a few counts per day per kg (cpd/kg) in the measured energy distributions mainly because of a contamination on the external surface of the Cu housing by environmental radon which occurred during the first period of the underground storage of the detectors.

The electronic trigger is issued when at least one crystal fires; then the pulse shape profile is acquired by a 200 MSample/s Lecroy Transient Digitizer if the event is a single hit in the lowest energy region; ADC values are recorded for each event in the whole energy scale [3].

A hardware/software stability monitoring system is operating; in particular, several probes are read out by the data acquisition system and stored with the production data. Moreover, self-controlled computer processes are operational to automatically control several parameters and to manage alarms.

The cumulative DAMA/NaI-3 and DAMA/NaI-4 energy spectrum between 1 to 10 keV has been reported in [7,11], while in [4,5,10–12] differential counting rates measured in various energy regions have also been shown. Here Fig. 2 has the aim to focus the energy spectra of the nine 9.7 kg NaI(Tl) detectors near the 2 keV software energy threshold; noise rejection procedures and correction for efficiency (see, e.g., [3] and Sect. 3.3) have already been applied. As usual in our experiment, the low energy distributions refer to those events where only one detector of many actually fires (that is, each detector had all the others in the same installation as veto; this assures a significant background reduction, which is obviously impossible when a single detector is used).

A typical behaviour with energy of the energy resolution is shown in Fig. 3. External gamma sources have been considered down to 59.5 keV (the line of ^{241}Am), while in-

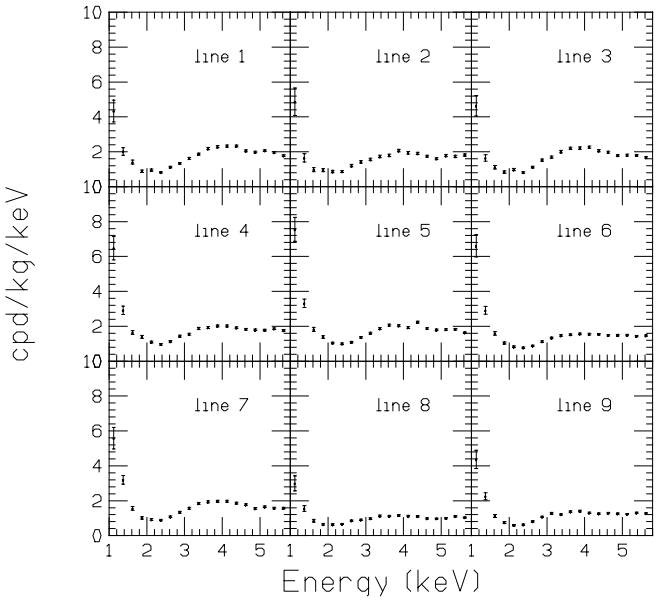

Fig. 2. Energy spectra (DAMA/NaI-3 and DAMA/NaI-4 data) of the nine detectors, used in the studies on the annual modulation signature, near the 2 keV software energy threshold (see text)

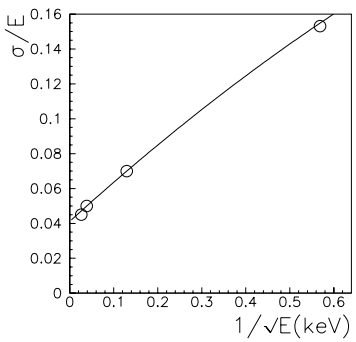

Fig. 3. Behaviour of the energy resolution for one of the used detectors as a function of the inverse of the squared root of the energy. A fit to the data points is shown; see text

ternal radiation has been considered in the keV energy region (external keV sources would be affected instead by energy degradation in the MIB window and surface roughness). The slight divergence from purely linear behaviour is consistent with a slight increase of the light response in the lowest energy region as measured by various authors since the '50s (see e.g. [13]).

3 The investigation of possible systematic effects

We have already presented elsewhere the results of the investigations of all the possible known sources of the systematics [3–5,7,6]; however, in the following a dedicated discussion on this topic will be carried out in a more extensive form, using for the quantitative examples the data of the DAMA/NaI-3 and DAMA/NaI-4 running periods which have more recently been released [7]. Similar arguments for DAMA/NaI-1 and DAMA/NaI-2 data have already been discussed elsewhere [4–6] and at many conferences and seminars. We further recall here that to mimic the annual modulation signature a systematic effect should not only be quantitatively significant, but should also be able to satisfy the six requirements as for a WIMP-induced effect (see Sect. 1).

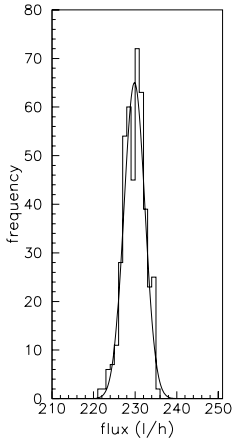

Fig. 4. Distribution of the HP nitrogen flux during both the DAMA/NaI-3 and DAMA/NaI-4 running periods

3.1 The radon

The environmental air contains traces of radioactive radon gas: ^{222}Rn ($T_{1/2} = 3.82$ days) and of ^{220}Rn ($T_{1/2} = 55$ s) isotopes, which belong to the ^{238}U and ^{232}Th chains, respectively. Moreover, their daughters attach themselves to surfaces by various processes. Therefore, the presence of a sizable quantity of radon near the detectors would forbid an annual modulation search because every radon variation would induce variation of the background measured by the detectors during the data taking. In addition, the exposed surfaces would be continuously polluted by the non-volatile daughters. It is, therefore, mandatory to efficiently exclude radon from the detectors.

On the other hand, when the annual modulation search is performed by experiments recording the whole energy spectrum (as in DAMA), the presence of a radon variation can be – in each case – identified, since it would induce a rate variation also in other energy regions than that of interest in WIMP search. Thus, we can conclude that, while the presence of radon forbids an annual modulation search, it cannot mimic the WIMP annual modulation signature since some of the six requirements for a WIMP-induced effect would fail.

In our set-up the detectors have been continuously isolated from environmental air since several years; in fact, the sealed Cu box housing them is maintained in the high purity nitrogen atmosphere (see Fig. 4) in slightly overpressure with respect to the environment. The low radioactivity multi-component shield surrounding the Cu box is also sealed in a plexiglass box and maintained in

HP nitrogen atmosphere. In addition, even the walls of the inner sealed barrack, where the set-up is installed, are covered by a Supronyl envelope (permeability: $2 \cdot 10^{-11}$ cm^2/s [9]) and a large flux of HP nitrogen is released in the close space of that inner barrack; an oxygen level alarm informs the operator before entering it, when necessary. The glove-box on the top of the installation is also maintained in the same HP nitrogen atmosphere in slightly overpressure [3]. Furthermore, the environmental radon level in the DAMA experimental area is continuously monitored and acquired with the production data (see Fig. 5); the results of the measurements are at the level of sensitivity of the used radonmeter. Finally, for the sake of completeness, we have examined the behaviour of the environmental radon level with time. When fitting the radon data with a cosine-like function having the period and phase expected for WIMPs, the values (0.14 ± 0.25) Bq/m^3 and (0.12 ± 0.20) Bq/m^3 are found for the modulation amplitude in the two periods respectively, both consistent with zero.

Notwithstanding the stringent operating conditions described above, we have also quantitatively investigated a possible presence of radon in the Cu box which is filled by detectors and Cu bricks as much as possible [3]. The possible radon concentration in the HP nitrogen atmosphere inside the Cu box has been estimated by searching for the double coincidences of the gamma-rays (609 and 1120 keV) from the ^{214}Bi radon daughter. An upper limit (90% C.L.) on the possible radon concentration in the Cu box atmosphere has been derived: $< 4.5 \cdot 10^{-2}$ Bq/m^3. By a Monte Carlo calculation it has been estimated that this limit gives in the lowest energy bins roughly $\lesssim 4 \cdot 10^{-4}$ cpd/kg/keV. Therefore, an hypothetical, e.g., 10% modulation of possible radon in the Cu box atmosphere would correspond to $< 0.2\%$ of the modulation amplitude we found in the lowest energy interval of the production data [4,5,7].

Finally, we remark that a modulation induced by radon – in every case – would always fail some of the six requirements of the annual modulation signature (such as, e.g., the 4th and the 5th), whose satisfaction is instead verified in the production data and, therefore, it would never mimic such a signature.

In conclusion, for all the arguments given above a radon effect can be excluded.

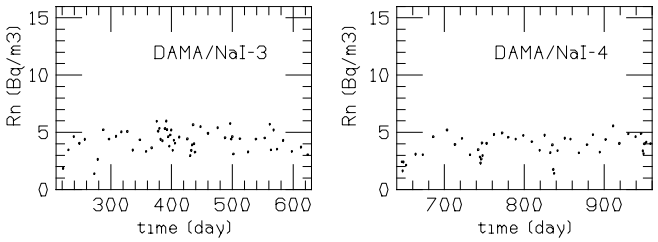

Fig. 5. Behaviour of the environmental radon inside the inner part of the barrack from which – as mentioned in the text – the detectors are excluded. The time scale starts January 1 1997

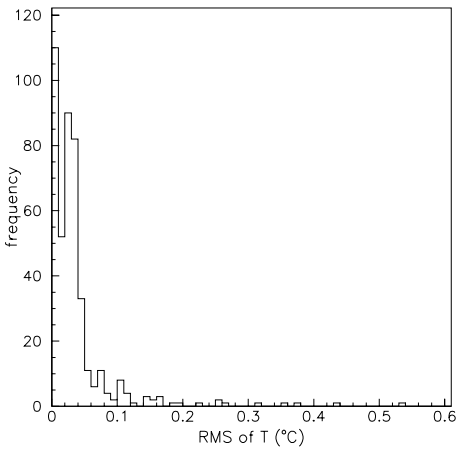

Fig. 6. Distribution of the root mean square temperature variation within periods with the same calibration factors (typically $\simeq$ 7 days). The mean value is 0.04°C

3.2 The temperature

To avoid any significant temperature variation and, in particular, to maintain suitably stable the temperature of the electronic devices, the installation where the $\simeq 100$ kg NaI(Tl) set-up is operating, is air-conditioned.

The operating temperature of the detectors in the Cu box is read out by a probe and it is stored with the production data [3–6,14]; this allows one to properly evaluate the real effect of possible temperature variations on the light output. For this purpose, the distribution of the root mean square temperature variation within periods with the same calibration factors (typically $\simeq$ 7 days) has to be considered; it is given in Fig. 6 for the DAMA/NaI-3 and DAMA/NaI-4 periods together. Considering its mean value ($\simeq 0.04$°C) and the value of the slope of the light output around our operating temperature ($\lesssim$ -0.2%/°C), the relative light output variation is $\lesssim 10^{-4}$. This corresponds to $\lesssim 0.5\%$ of the modulation amplitude observed in the lowest energy region of the production data as reported in [4,5,7].

Moreover, a time correlation analysis of the temperature data, including a modulated component with period and phase as for WIMPs, gives modulation amplitudes compatible with zero: (0.021 ± 0.046)°C and (0.064 ± 0.058)°C for DAMA/NaI-3 and DAMA/NaI-4, respectively.

For the sake of completeness, we comment that sizable temperature variations could also induce variations in the electronic noise, in the radon release from the rocks and, therefore, in the environmental background; these specific topics are analysed in Sects. 3.1, 3.3 and 3.6, where cautious upper limits of their possible effects are given.

Finally, it is worth to remark that every possible effect induced by temperature variations would fail at least some of the six requirements needed to mimic the annual modulation signature (such as, e.g., the 4th and the 5th).

In conclusion, all the arguments given above exclude any role of possible effects correlated with temperature.

3.3 The noise

The only data treatment which is performed on the raw data is to eliminate obvious noise events (whose number sharply decreases when increasing the number of available photoelectrons) present below $\simeq 10\,\mathrm{keV}$ [3]. The noise in our experiment is given by PMT fast single photoelectrons with decay times of the order of tens of ns, while the "physical" (scintillation) pulses have decay times of order of hundreds ns. The large difference in decay times and the relatively large number of available photoelectrons response assure an effective noise rejection [3]. As mentioned in [3,5] several variables can be built by using the pulse information recorded over 3250 ns by a Transient Digitizer. In particular, for each energy bin, we plot the

$$Y = \frac{\text{Area(from 0 ns to 50 ns)}}{\text{Area(from 0 ns to 100 ns)}}$$

value versus the

$$X = \frac{\text{Area(from 100 ns to 600 ns)}}{\text{Area(from 0 ns to 600 ns)}}$$

value calculated for every event. In the X, Y plane the slow scintillation pulses are grouped roughly around ($X \simeq 0.7$, $Y \simeq 0.5$), well separated from the noise population which is grouped around small X and high Y values (see [3,5]). To select the scintillation pulses an acceptance window in X, Y is applied. Since the statistical spread of the two populations in the X, Y plane becomes larger when the number of available photoelectrons and the signal/noise ratio decrease, windows with smaller acceptance become necessary to maintain the same noise rejection power. In our experiment they are kept stringent enough to assure also the absence of any possible residual noise tail in the scintillation data to be analysed (this should be necessary also, e.g., for correct pulse shape discrimination) [3]. According to standard procedures, the acceptance of the considered window for scintillation pulses in the X, Y plane is determined by applying the same procedure to the scintillation data induced – in the same energy interval – by an external source of suitable strength [3,7]. The acceptance values are generally in our papers called cut efficiencies[2]. As already mentioned, the single hit energy spectrum given by the sum of the scintillation pulses and of the noise pulses (to be rejected) is of order of $\simeq 10\,\mathrm{cpd/kg/keV}$ near the used software energy threshold; it sharply decreases with the increase of the available number of photoelectrons. This is a favourable situation; however, as mentioned above, stringent windows are set in the X, Y plane at low energy to achieve a full noise rejection since the acceptance can be determined with high accuracy [7]. Slightly different choices give substantially the same results. The acceptance values are equal to unity above $\simeq 8\,\mathrm{keV}$ [3].

Notwithstanding the described procedure, we have also quantitatively investigated the role played in the studies of the annual modulation signature by possible noise tail in the data after noise rejection. The hardware rate of each one of the nine detectors above a single photoelectron, R_{Hj} (j identifies the detector), can be considered; in fact, it is significantly determined by the noise. For this purpose the variable $R_H = \Sigma_j(R_{Hj} - < R_{Hj} >)$ can be built (where in our case $\langle R_{Hj} \rangle \lesssim 0.25\,\mathrm{Hz}$ [3]); its time behaviour during the DAMA/NaI-3 and the DAMA/NaI-4 running periods is shown in Fig. 7. As can be seen in Fig. 8, the distribution of R_H shows a gaussian behaviour with $\sigma = 0.6\%$ and 0.4% for DAMA/NaI-3 and DAMA/NaI-4, respectively, values well in agreement with those expected

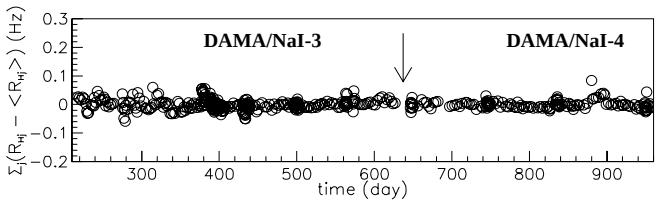

Fig. 7. Time behaviour of R_H; see text. The time scale here starts from January 1 1997

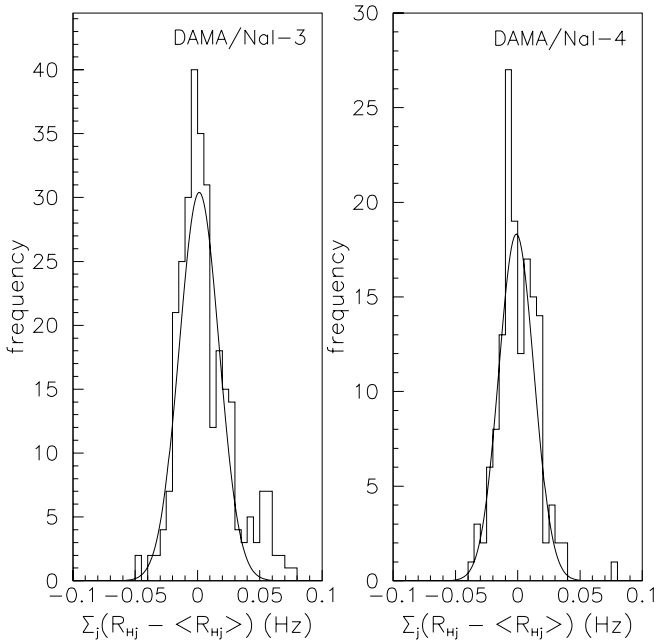

Fig. 8. Distributions of R_H (see text)

[2] For non-expert readers, we recall that the noise peculiarities depend on the specific PMTs, voltage dividers, electronic noise features, hardware setting etc. Therefore the quantitative values of the used windows have no practical utility for other experiments. Furthermore, the shape of the energy spectra after noise rejection depends on the effectiveness of the noise rejection procedures and on the residual contaminants in the used detector and installation. As an example, we mention that in our case the single hit energy spectrum given by the sum of the scintillation events and of the noise events (to be rejected) is at level of $\simeq 9$ counts per day per kg per keV (or lower, depending on the detector) around 3 keV. This rate is similar to the one quoted in [23] only after a noise rejection procedure; therefore, e.g., the $\simeq 2.5\,\mathrm{keV}$ peak (whose real nature has never been unambiguously clarified by the authors) found there [23] is not present in our data, whatever noise rejection procedure would be applied. See in addition Sect. 4

on the basis of simple statistical arguments. Moreover, by fitting the time behaviour of R_H in both data periods – including a WIMP-like modulated term – a modulation amplitude compatible with zero, $(0.04 \pm 0.12) \cdot 10^{-2}$ Hz, is obtained. From this value the upper limit at 90% C.L. on the modulation amplitude can be derived: $< 1.6 \cdot 10^{-3}$ Hz. Since the typical noise contribution to the hardware rate of each one of the nine detectors is $\simeq 0.10$ Hz, the upper limit on the noise relative modulation amplitude is given by $1.6 \cdot 10^{-3}$ Hz$/9 \times 0.10$ Hz $\simeq 1.8 \cdot 10^{-3}$ (90% C.L.). Therefore, even in the worst hypothetical case of a 10% contamination of the residual noise – after rejection – in the counting rate, the noise contribution to the modulation amplitude in the lowest energy bins would be $< 1.8 \cdot 10^{-4}$ of the total counting rate. This means that a possible noise modulation can account at maximum for absolute amplitudes of the order of few 10^{-4} cpd/kg/keV, that is $< 1\%$ of the observed annual modulation amplitude [7].

In conclusion, there is no evidence for any role of an hypothetical tail of residual noise after rejection.

3.4 The calibration factor

As mentioned in Sect. 2, in long term running conditions, the knowledge of the energy scale is assured by periodical calibration with a ^{241}Am source and by continuously monitoring within the same production data (grouping them each $\simeq 7$ days) the position and resolution of the ^{210}Pb peak (46.5 keV) [3–5,7]. Although it is highly unlikely that a variation of the calibration factor (proportionality factor between the area of the recorded pulse and the energy), *tdcal*, could mimic the annual modulation signature satisfying the six requirements for a WIMP-induced effect, we present in the following a quantitative investigation on that point according to [3,5,7,6].

For this purpose, the distributions of the relative variations of *tdcal* – without applying any correction – estimated from the position of the ^{210}Pb peak for all the nine detectors during both the DAMA/NaI-3 and the DAMA/NaI-4 running periods, have been investigated; see Fig. 9. These distributions show a gaussian behaviour with $\sigma \lesssim 1\%$. Since the results of the routine calibrations are obviously properly taken into account in the data analysis, such a result allows us to conclude that the energy calibration factor for each detector is known with an uncertainty $\ll 1\%$ within every 7 days interval.

Moreover, the variation of the calibration factor for each detector, within each interval of $\simeq 7$ days, would give rise to an additional energy spread ($\sigma_{\rm cal}$) besides the detector energy resolution ($\sigma_{\rm res}$). Therefore, the total energy spread can be written as

$$\sigma = (\sigma_{\rm res}^2 + \sigma_{\rm cal}^2)^{1/2} \simeq \sigma_{\rm res} \cdot \left[1 + \frac{1}{2} \cdot \left(\frac{\sigma_{\rm cal}}{\sigma_{\rm res}}\right)^2\right],$$

and the contribution due to the calibration factor variation is negligible since

$$\frac{1}{2} \cdot \left(\frac{\sigma_{\rm cal}/E}{\sigma_{\rm res}/E}\right)^2 \lesssim 7.5 \cdot 10^{-4} \frac{E}{20\,{\rm keV}},$$

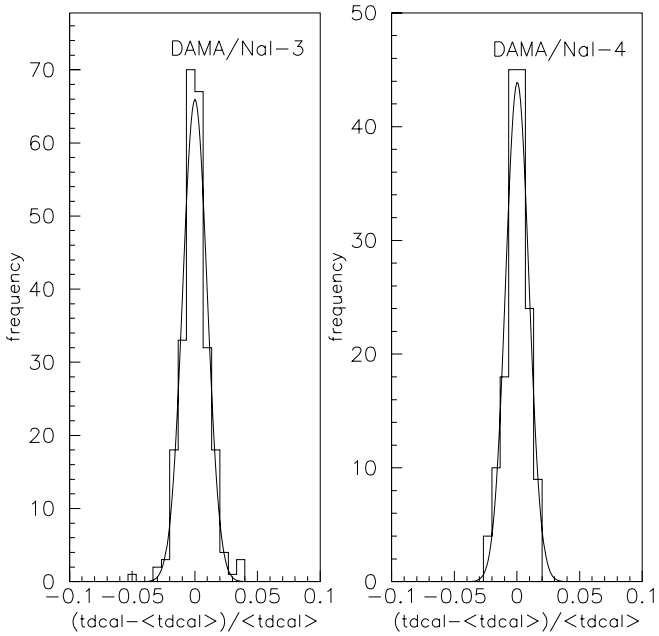

Fig. 9. Distribution of the percentage variations of the energy scale factors (*tdcal*) with respect to their mean values for all the detectors without applying any correction (see text). The standard deviations are (0.98 ± 0.05)% and (0.92 ± 0.09)%, respectively

where the adimensional ratio $E/20$ keV accounts for the energy dependence of this limit value. This order of magnitude is confirmed by a Monte Carlo calculation, where the effect of similar variations of *tdcal* on the modulation amplitude has been estimated; in fact, its maximum value as a results is there $1.6 \cdot 10^{-4}$ and gives an upper limit of $< 1\%$ of the modulation amplitude measured at very low energy in [4,5,7].

3.5 The efficiencies

The behaviour of the used efficiencies during the whole data taking periods has even been investigated. Their possible time variation depends essentially on the stability of the cut efficiencies (see Sect. 3.3), which are regularly measured by dedicated calibrations [3,5,7].

In particular, we show in Fig. 10 the percentage variations of the efficiency values in the (2–8) keV energy interval considering 2 keV bins. They show a gaussian distribution with $\sigma = 0.6\%$ and 0.5% for DAMA/NaI-3 and DAMA/NaI-4, respectively. Moreover, we have verified that the time behaviour of these percentage variations does not show any modulation with period and phase expected for a possible WIMP signal. In particular, in the (2–4) keV energy interval a modulation amplitude (taking the two periods all together) equal to $(1.0 \pm 1.0) \cdot 10^{-3}$ is found, while in the (4–6) keV the result is $(0.1 \pm 0.7) \cdot 10^{-3}$; they are both consistent with zero. Similar results are obtained in other energy bins.

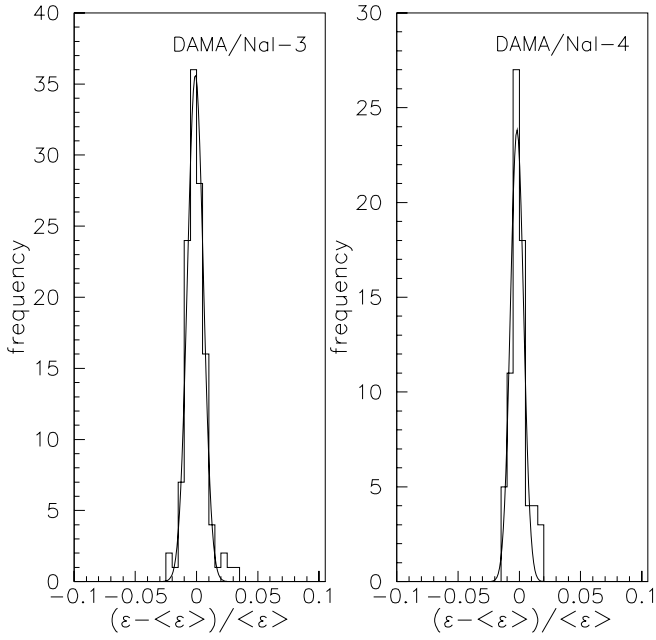

Fig. 10. Distribution of the percentage variations of the efficiency with the respect to their mean values for all the detectors; see text

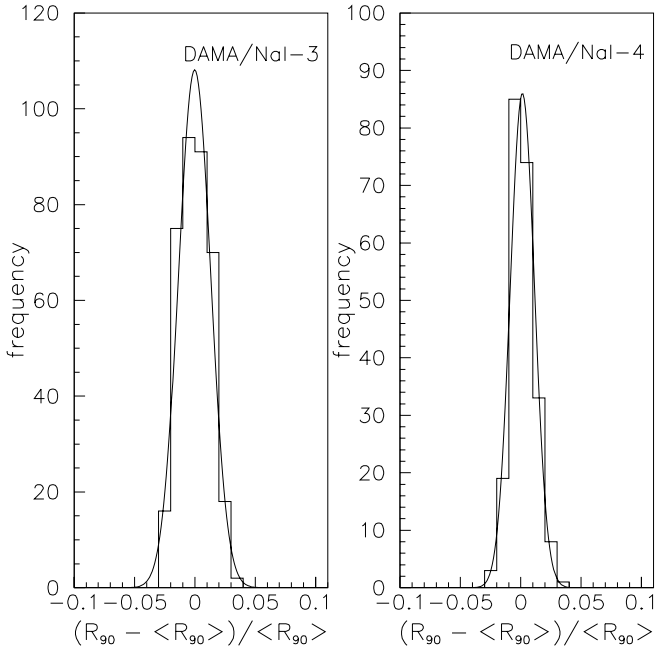

Fig. 11. Distributions of the percentage variations of R_{90} with respect to their mean values for all the detectors; see text

Therefore, also the unlikely idea of a possible role played by the efficiency values in the effect observed in [4,5,7] has been ruled out.

3.6 The background

In order to verify the absence of any significant background modulation, the energy distribution measured during the data taking in energy regions not of interest for the WIMP–nucleus elastic scattering has been investigated in order to verify if the modulation detected in the lowest energy region [4–7] could be ascribed to a background modulation. In fact, the background in the lowest energy region can be essentially due to "Compton" electrons, X-rays and/or Auger electrons, muon-induced events, etc., which are strictly correlated with the events in the higher energy part of the spectrum. Therefore, if a modulation with time detected in the lowest energy region would be due to a modulation of the background (instead of the possible signal) with time, an equal or larger (sometimes much larger) modulation in the higher energy regions should be present. For this purpose, we have investigated the rate integrated above 90 keV, R_{90}, as a function of time. In Fig. 11 the distributions of the percentage variations of R_{90} with respect to their mean values for all the nine detectors during the whole DAMA/NaI-3 and DAMA/NaI-4 running periods are given. They show cumulative gaussian behaviours with $\sigma \simeq 1\%$, well accounted by the statistical spread expected from the used sampling time. This result excludes any significant background variation.

Moreover, fitting the time behaviour of R_{90}, a WIMP-like modulation amplitude compatible with zero is found in both the running periods: $-(0.11 \pm 0.33)$ cpd/kg and $-(0.35 \pm 0.32)$ cpd/kg, respectively. This excludes the presence of a background modulation in the whole energy spectrum at a level much lower than the effect found in the lowest energy region in [4,5,7]; in fact, otherwise – considering the R_{90} mean values – its modulated term should be of order of tens cpd/kg, that is, $\simeq 100\sigma$ away from the measured value.

A similar analysis can be performed in the energy region just above the first pole of the iodine form factor: again, modulation amplitudes of the counting rate statistically compatible with zero have been found. In fact, in the energy region 10–20 keV they are $-(0.0044 \pm 0.0044)$ cpd/kg/keV and $-(0.0071 \pm 0.0044)$ cpd/kg/keV for the two periods, both statistically compatible with zero. Moreover, performing similar calculations for the (6–10) keV energy interval one gets $-(0.0017 \pm 0.0037)$ cpd/kg/keV for the two periods together.

Notwithstanding that the results given above already account also for the background component due to the environmental neutrons, we will present in the following a further additional independent analysis to estimate the possible contribution arising from the environmental neutrons.

As regards the thermal neutrons, the reactions $^{23}\mathrm{Na}(n,\gamma)^{24}\mathrm{Na}$ and $^{23}\mathrm{Na}(n,\gamma)^{24m}\mathrm{Na}$ (cross section to thermal neutrons equal to 0.10 and 0.43 barn, respectively [15]) have been investigated. The capture rate as a result is found to be $\simeq 0.2$ captures/day/kg since the thermal neutron flux has been measured to be $1.08 \cdot 10^{-6}$ neutrons cm^{-2} s^{-1} [16][3]. Assuming cautiously a 10% modula-

[3] A consistent upper limit on the thermal neutron flux has been obtained with the $\simeq 100$ kg DAMA NaI(Tl) set-up considering these same capture reactions [3]

tion of the thermal neutrons flux, the corresponding modulation amplitude in the lowest energy region has been calculated by a Monte Carlo program to be $< 10^{-5}$ cpd/kg/keV, that is $< 0.05\%$ of the modulation amplitude we found in the lowest energy interval of the production data. In addition, a similar contribution cannot anyhow mimic the annual modulation signature since it would fail some of the six requirements quoted in Sect. 1 (such as, e.g., the 4th and the 5th).

A similar analysis can also be carried out for the fast neutron case. From the fast neutron flux measured at the Gran Sasso underground laboratory, $0.9 \cdot 10^{-7}$ neutrons cm^{-2} s^{-1} [17], the differential counting rate above 2 keV has been estimated by Monte Carlo to be $\simeq 10^{-3}$ cpd/kg/keV. Therefore, cautiously assuming – also in this case – a 10% modulation of the fast neutron flux, the corresponding modulation amplitude as a result is found to be $< 0.5\%$ of the modulation amplitude found in the lowest energy interval in [4,5,7]. Moreover, also in this case some of the six requirements mentioned above would fail.

In conclusion, the results presented in this section demonstrate that the production data satisfy the 4th requirement quoted in Sect. 1 and – at the same time – exclude that the annual modulation observed in the lowest energy region in [4,5,7] could be ascribed to background modulation.

3.7 The side reactions

Possible side reactions have been also carefully searched for. The only process which has been found so far as an hypothetical possibility is the muon flux modulation reported by the MACRO experiment [18]. In fact, MACRO has observed that the muon flux shows a nearly sinusoidal time behaviour with one year period and maximum in the summer with amplitude of $\simeq 2\%$; this muon flux modulation is correlated with the temperature of the atmosphere.

A simple calculation can be performed to estimate the modulation amplitude expected from this process in our set-up. For this purpose, the muon flux (Φ_μ) and the yield of neutrons produced by muons measured at the underground Gran Sasso National Laboratory (Y) have to be taken into account; they are $\Phi_\mu \simeq 20$ muons m^{-2}d^{-1} [18] and $Y \simeq (1\text{–}7) \cdot 10^{-4}$ neutrons per muon per g/cm^2 [19], respectively. The fast neutron rate produced by muons is given by: $R_n = \Phi_\mu \cdot Y \cdot M_{\rm eff}$, where $M_{\rm eff}$ is the effective mass where muon interactions can give rise to events detected in the DAMA set-up. Therefore, as regards our experiment, the annual modulation amplitude in the lowest energy region due to a muon flux modulation as measured by MACRO [18] can be expressed according to $S_m^{(\mu)} = R_n \cdot g \cdot \epsilon \cdot f_{\Delta E} \cdot f_{\rm single} \cdot 2\%/(M_{\rm set-up} \cdot \Delta E)$, where g is a geometrical factor, ϵ is the detection efficiency for elastic scattering interactions, $f_{\Delta E}$ is the acceptance of the considered energy window (E $\geq$ 2 keV), $f_{\rm single}$ is the "single hit" efficiency and 2% is the MACRO measured effect. Since $M_{\rm set-up} \simeq 100$ kg and $\Delta E \simeq 4$ keV, assuming the very cautious values $g \simeq \epsilon \simeq f_{\Delta E} \simeq f_{\rm single} \simeq 0.5$ and $M_{\rm eff} = 15$ t, one obtains $S_m^{(\mu)} < (1\text{–}7) \cdot 10^{-5}$ cpd/kg/keV, that is, $< 0.3\%$ of the modulation amplitude we observe [7].

In conclusion, the modulation of the muon flux observed by MACRO cannot account for the effect we have observed in [4,5,7] since it would give rise in our set-up to a quantitatively negligible effect and – in addition – some of the six requirements necessary to mimic the annual modulation signature (such as, e.g., the 4th and the 5th) would fail. Therefore, it can be safely ignored.

The search for other possible side reactions able to mimic the signature has not offered so far any candidate.

4 Some satellite arguments

We take this opportunity to briefly comment on the so-called "anomalous" events observed by other groups in their NaI(Tl) experimental set-ups during their pulse shape discrimination (PSD) procedures [21,23] (we recall that no PSD at all has been applied to the data we have used in the annual modulation studies for the reasons mentioned, e.g., in [4]).

In 1998 (about 2 years later than our study on PSD [8] and the first UK collaboration PSD result [20]) the UK collaboration claimed presence in its new data of pulses (called "anomalous") with decay time shorter than those induced by recoiling nuclei up to about 100 keV [21,22]; afterwards, similar pulses (called "unknown") were claimed also in [23][4]. No conclusive statement on the real origin of these events was set by the authors.

In our experiment similar events have never been observed. In particular, their presence was already excluded since [8]; in fact, the PSD analysis method used there was able to point out similar events since they would mimic the presence of a sizable number of recoils. In Fig. 12 the upper limits we measured in our [8] are compared with the "anomalous" or "unknown" event rates quoted later by the two mentioned collaborations.

[4] This latter group realised two detectors similar in shape to our ones by using – as far as we know – in total or in part some spare parts of a bulk material grown more than one year before for some of our ten detectors (only nine used in the $\simeq 100$ kg NaI(Tl) set-up). The drawbacks in using bulk material stored for long at sea level in normal industrial conditions can be easily inferred as well as the obvious different cutting, polishing, assembling and handling procedures. Moreover, all the other materials used to realise these detectors (such as Cu housing, light guides, etc.) cannot come from the same batch as our ones. As is widely known in the field of low radioactivity experiments, the role of different history of the detectors, of different storage procedures in time, of different exposures to natural and artificial radioactivity (as, e.g., neutron sources and cosmogenic activation), of different features in different installations (residual contaminations in the nearby materials, radon removal effectiveness and continuity, etc.) is highly relevant. The large improvement in energy resolution of the detector used in [23] with respect to our own detectors (which cannot be explained by differences in PMT quantum efficiency, since they are marginal) is another remarkable difference

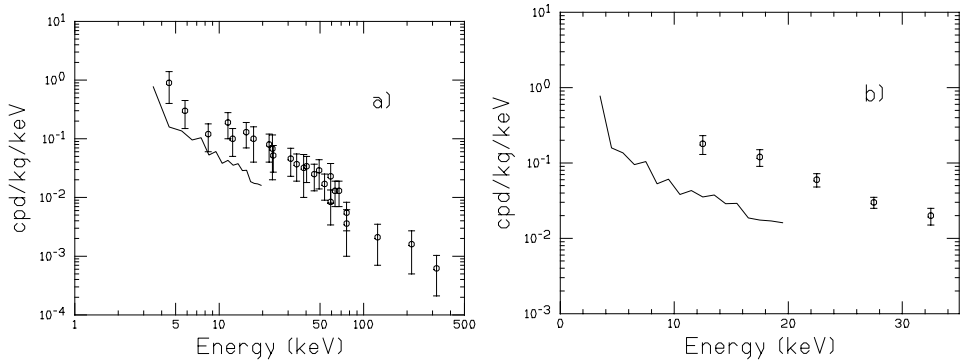

Fig. 12a,b. Comparison of the upper limits we measured in [8] (continuous line) with the rate of "anomalous" **a** and "unknown" **b** events measured in [24] and in [23], respectively

As is known, pulses like the so-called "anomalous" or "unknown" ones could be induced by various known systematic effects, such as:

(1) unsuitable hardware setting for afterglow rejection;
(2) significant contribution from Cherenkov pulses in the light guides which induce light pulses in the NaI(Tl), giving events with shortened decay time;
(3) a not suitably controlled temperature stability in the Compton and/or neutron and/or production data (we recall that the pulse shape in NaI(Tl) has a significant dependence on temperature); etc.

For the sake of completeness, we recall that a possible huge U/Th contamination (much higher than the bulk content) of the surfaces of the detectors used by these experiments has also been hypothesised as an explanation, but has been considered highly unlikely [25]. Various authors have also considered that processes induced by huge radon contamination [25–27] could account for those "anomalous" or "unknown" events. Also this hypothesis can match with our observation of absence of similar events in our experiment, since, e.g.,

(1) our detectors have been assembled just after the growth of the crystalline bulk in a glove-box, tightly sealed and immediately brought underground;
(2) microcracks in the housings of our detectors are absent having, e.g., no presence of any light degradation during several years;

(3) our detectors are tightly enclosed in thick Cu housings and are continuously maintained since several years in HP nitrogen atmosphere, where the possible radon concentration has been measured to be $< 4.5 \cdot 10^{-2}$ Bq/m^3 (90% C.L.) as discussed in Sect. 3.1.

Moreover, as a general comment, we note that any hypothetical contribution from the ^{214}Po radon daughter implanted on the crystal surface [27] would be strongly suppressed in DAMA by the veto of ^{214}Bi–^{214}Po delayed coincidences performed by the typical DAMA acquisition duty cycle [3].

In conclusion, for the arguments of this and of previous section, no role is present in our experiment for so-called "anomalous" or "unknown" events.

5 Conclusions and implications on the annual modulation result

The quantitative investigations discussed above offer a complete analysis of known sources of possible systematic effects. We can conclude that a relative systematic error, affecting the energy spectrum, of order of $\lesssim 10^{-3}$ is credited by these investigations, while the results on the analysis of R_{90} exclude the presence of a possible background modulation even at more stringent level. Furthermore, no systematic effect or side reaction able to mimic a WIMP-induced effect, also satisfying – as necessary – all the six requirements quoted in Sect. 1, have been found so far.

In conclusion, the result of the model independent approach [7], summarised in Sect. 1, together with the result of this search for possible systematics able to mimic the WIMP annual modulation signature, supports the presence of a possible WIMP contribution to the measured rate independently on the nature and coupling with ordinary matter of the involved candidate. For the sake of completeness we recall that a full energy and time correlation analysis – accounting also for the constraint arising from [8] – has been carried out in [7] in the framework of a particular model for spin independent coupled candidates with mass above 30 GeV [4,5,7]. In [28] the theoretical implications in terms of neutralino with a dominant spin independent interaction and mass above 30 GeV have been discussed, while the case for a heavy neutrino of the fourth family has been introduced in [29].

The data of a fifth annual cycle are under analysis. Furthermore, investigations of the role played by the uncertainties on several physical parameters and on the assumptions needed in the calculations are in progress as well as investigations of possible different model dependent scenarios.

During the next annual cycle a new electronics and DAQ will be operative. Moreover, since a new dedicated R&D has been completed, the exposed mass is in progress to be enlarged up to $\simeq$ 250 kg in order to increase the experimental sensitivity.

References

1. K.A. Drukier, et al., Phys. Rev. D **33**, 3495 (1986)
2. K. Freese, et al., Phys. Rev. D **37**, 3388 (1988)

3. R. Bernabei, et al., Il Nuovo Cimento A **112**, 545 (1999)
4. R. Bernabei, et al., Phys. Lett. B **424**, 195 (1998)
5. R. Bernabei, et al., Phys. Lett. B **450**, 448 (1999)
6. P. Belli, et al., in 3K-Cosmology (AIP pub., 65, 1999)
7. R. Bernabei, et al., Phys. Lett. B **480**, 23 (2000)
8. R. Bernabei, et al., Phys. Lett. B **389**, 757 (1996)
9. M. Wojcik, Nucl. Instrum. Methods B **61**, 8 (1991)
10. P. Belli, et al., Phys. Lett. B **460**, 236 (1999)
11. R. Bernabei, et al., Il Nuovo Cimento A **112**, 1541 (1999)
12. P. Belli, et al., Phys. Rev. C **60**, 065501 (1999)
13. J.B. Birks, Theory and practice of scintillation counters (Pergamon Press, Oxford 1964)
14. R. Bernabei, et al., ROM2F/2000-15 to appear on the Proceedings of International workshop DM2000, Marina del Rey, Usa, February 2000
15. Table of Isotopes, edited by C.M. Lederer, V.S. Shirley, 7th ed. (John Wiley, New York 1978)
16. P. Belli, et al., Il Nuovo Cimento A **101**, 959 (1989)
17. M. Cribier, et al., Astropart. Phys. **4**, 23 (1995)
18. M. Ambrosio, et al., Astropart. Phys. **7**, 109 (1997)
19. M. Aglietta, et al., Il Nuovo Cimento C **12**, 467 (1987); hep-ex/9905047
20. P.F. Smith, et al., Phys. Lett. B **379**, 299 (1996)
21. N. Spooner: in Proceedings of the 6th International Symposium Particles, Strings and Cosmology, edited by P. Nath (World Scientific, 1999), p. 130
22. V.A. Kundryavtsev, et al., Phys. Lett. B **452**, 167 (1999)
23. G. Gerbier, et al., Astropart. Phys. **11**, 287 (1999)
24. I. Liubarsky, et al., Nucl. Phys. B (Proc. Suppl.) **87**, 64 (2000)
25. N.J.T. Smith, et al., Phys. Lett. B **485**, 9 (2000)
26. G. Chardin, et al., Nucl. Phys. B (Proc. Suppl.) **87**, 74 (2000)
27. S. Cooper, et al., Phys. Lett. B **490**, 6 (2000)
28. A. Bottino, et al., hep-ph/0001309 to appear in Phys. Rev. D; Phys. Lett. B **402**, 113 (1997); Phys. Lett. B **423**, 109 (1998); Phys. Rev. D **59**, 095004 (1999); Phys. Rev. D **59**, 095003 (1999); Astropart. Phys. **10**, 203 (1999); Astropart. Phys. **13**, 215 (2000); R.W. Arnowitt, P. Nath, Phys. Rev. D **60**, 044002 (1999)
29. D. Fargion, et al., Pis'ma Zh. Eksp. Teor. Fiz. **68**, (JETP Lett. 68, 685) (1998); Astropart. Phys. **12**, 307 (2000)